Editorial Manager(tm) for Biomaterials
Manuscript Draft

Manuscript Number:

Title: Effects of incorporation of poly(γ-glutamic acid) in chitosan/DNA complex nanoparticles on enhancing their cellular uptake and transfection efficiency

Article Type: FLA Original Research

Section/Category: Biomaterials & Gene Transfer

Keywords: chitosan; poly(γ-glutamic acid); transfection efficiency; cellular uptake

Corresponding Author: Dr. Hsing-Wen Sung,

Corresponding Author's Institution: National Tsing Hua University

First Author: Shu-Fen Peng

Order of Authors: Shu-Fen Peng; Mei-Ju Yang; Chun-Jen Su; Hsin-Lung Chen; Po-Wei Lee; Ming-Cheng Wei; Hsing-Wen Sung

Abstract: Chitosan (CS)/DNA complex nanoparticles (NPs) have been considered as a vector for gene delivery. Although advantageous for DNA packing and protection, CS-based complexes may lead to difficulties in DNA release once arriving at the site of action. In this study, a new approach through modifying their internal structure by incorporating a negatively charged poly(γ-glutamic acid) (γ-PGA) in CS/DNA complexes (CS/DNA/γ-PGA NPs) is reported. The analysis of small angle X-ray scattering results revealed that DNA and γ-PGA formed complexes with CS separately to yield two types of domains, leading to the formation of "compounded NPs". With this unique internal structure, the compounded NPs might disintegrate into a number of even smaller sub-particles after cellular internalization, thus improving the dissociation capacity of CS and DNA. Consequently, after incorporating γ-PGA in CS/DNA complexes, a significant increase in their transfection efficiency was found. Interestingly, in addition to improving the release of DNA intracellularly, the

incorporation of γ-PGA in CS/DNA complexes significantly enhanced their cellular uptake. We further demonstrated that besides a non-specific charged-mediated binding to cell membranes, there were specific trypsin-cleavable proteins involved in the internalization of CS/DNA/γ-PGA NPs. The aforementioned results indicated that γ-PGA played multiple important roles in enhancing the cellular uptake and transfection efficiency of CS/DNA/γ-PGA NPs.

* Mandatory Author Declaration

AUTHOR DECLARATION TEMPLATE

We the undersigned declare that this manuscript is original, has not been published before and is not currently being considered for publication elsewhere.

We wish to draw the attention of the Editor to the following facts which may be considered as potential conflicts of interest and to significant financial contributions to this work. [OR]
We wish to confirm that there are no known conflicts of interest associated with this publication and there has been no significant financial support for this work that could have influenced its outcome.

We confirm that the manuscript has been read and approved by all named authors and that there are no other persons who satisfied the criteria for authorship but are not listed. We further confirm that the order of authors listed in the manuscript has been approved by all of us.

We confirm that we have given due consideration to the protection of intellectual property associated with this work and that there are no impediments to publication, including the timing of publication, with respect to intellectual property. In so doing we confirm that we have followed the regulations of our institutions concerning intellectual property.

We understand that the Corresponding Author is the sole contact for the Editorial process (including Editorial Manager and direct communications with the office). He/she is responsible for communicating with the other authors about progress, submissions of revisions and final approval of proofs. We confirm that we have provided a current, correct email address which is accessible by the Corresponding Author and which has been configured to accept email from biomaterials@online.be.

Signed by all authors as follows:

[LIST AUTHORS AND DATED SIGNATURES ALONGSIDE]

Shu-Fen Peng Shu-Fen Peng 10/3/2008.

Mei-Ju Yang Mei-Ju Yang 10/3/2008

Chun-Jen Su Chun-Jen Su 10/3 2008.

Hsin-Lung Chen Hsin-Lung Chen 10/3/2008

Po-Wei Lee Po-Wei Lee. 10/3/2008.

Ming-Cheng Wei Ming-Cheng Wei 10/3/2008

Hsing-Wen Sung Hsing-Wen Sung 10/3/2008

October 3, 2008

Professor D. F. Williams
Editor-in-Chief
Biomaterials

Dear Professor Williams:

Attached please find a manuscript entitled "Effects of incorporation of poly(γ-glutamic acid) in chitosan/DNA complex nanoparticles on enhancing their cellular uptake and transfection efficiency". The manuscript is intended to be published in *Biomaterials*. It has been sorely submitted to *Biomaterials* and that it is not concurrently under consideration for publication in any other journal. We believe these results are of very broad significance and hope you will consider reviewing the manuscript. We value you and the reviewers' suggestions and comments.

Sincerely yours,

Hsing-Wen Sung, Ph.D.
Professor
Department of Chemical Engineering/Bioengineering Program
National Tsing Hua University
Hsinchu, Taiwan 30013
Phone: +886-3-574-2504
Fax: +886-3-572-6832
Email: hwsung@che.nthu.edu.tw

Impact Statement:

Chitosan (CS)/DNA complex nanoparticles (NPs) have been considered as a vector for gene delivery; however, CS-based complexes may lead to difficulties in DNA release once arriving at the site of action. In this study, a new approach through modifying their internal structure by incorporating a negatively charged poly(γ-glutamic acid) (γ-PGA) in CS/DNA complexes is reported. We demonstrated that DNA and γ-PGA formed complexes with CS separately to yield two types of domains, leading to the formation of "compounded NPs". With this unique internal structure, the compounded NPs might disintegrate into a number of even smaller sub-particles after cellular internalization, thus improving the dissociation capacity of CS and DNA. Interestingly, in addition to improving the release of DNA intracellularly, the incorporation of γ-PGA in CS/DNA NPs significantly enhanced their cellular uptake. Taken together, γ-PGA significantly enhanced the transfection efficiency of this newly developed gene-delivery system.

Effects of incorporation of poly(γ-glutamic acid) in chitosan/DNA complex nanoparticles on enhancing their cellular uptake and transfection efficiency

Shu-Fen Peng[1], Mei-Ju Yang[1,2], Chun-Jen Su[1], Hsin-Lung Chen[1]
Po-Wei Lee[1], Ming-Cheng Wei[1], Hsing-Wen Sung[1*]

[1] Department of Chemical Engineering, National Tsing Hua University, Hsinchu, Taiwan, R.O.C.

[2] Biomedical Engineering Research Laboratories, Industrial Technology Research Institute, Hsinchu, Taiwan, R.O.C.

[*]**Correspondence to:**
Hsing-Wen Sung, PhD
Professor
Department of Chemical Engineering/Bioengineering Program
National Tsing Hua University
Hsinchu, Taiwan 30013
Tel: +886-3-574-2504
Fax: +886-3-572-6832
E-mail: hwsung@che.nthu.edu.tw

Abstract

Chitosan (CS)/DNA complex nanoparticles (NPs) have been considered as a vector for gene delivery. Although advantageous for DNA packing and protection, CS-based complexes may lead to difficulties in DNA release once arriving at the site of action. In this study, a new approach through modifying their internal structure by incorporating a negatively charged poly(γ-glutamic acid) (γ-PGA) in CS/DNA complexes (CS/DNA/γ-PGA NPs) is reported. The analysis of small angle X-ray scattering results revealed that DNA and γ-PGA formed complexes with CS separately to yield two types of domains, leading to the formation of "compounded NPs". With this unique internal structure, the compounded NPs might disintegrate into a number of even smaller sub-particles after cellular internalization, thus improving the dissociation capacity of CS and DNA. Consequently, after incorporating γ-PGA in CS/DNA complexes, a significant increase in their transfection efficiency was found. Interestingly, in addition to improving the release of DNA intracellularly, the incorporation of γ-PGA in CS/DNA complexes significantly enhanced their cellular uptake. We further demonstrated that besides a non-specific charged-mediated binding to cell membranes, there were specific trypsin-cleavable proteins involved in the internalization of CS/DNA/γ-PGA NPs. The aforementioned results indicated that γ-PGA played multiple important roles in enhancing the cellular uptake and transfection efficiency of CS/DNA/γ-PGA NPs.

Keywords: chitosan; poly(γ-glutamic acid); transfection efficiency; cellular uptake

1. Introduction

Chitosan (CS), a cationic polysaccharide, is biodegradable, non-toxic and tissue compatible [1–4]. It has the potential to condense anionic DNA into a compact structure through electrostatic interactions and has been considered to be a good candidate as non-viral vectors [5–7]. CS/DNA complexes can be readily prepared to provide an effective protection against DNase [8,9]. CS/DNA complexes generally transfect cells more efficiently than naked DNA but less than commercially available liposome formulations. It has been suggested that the strength of electrostatic interactions between CS and DNA prevent their dissociation within cells, thus precluding transcription of DNA and resulting in low transfection [10].

To improve the transfection efficiency of CS/DNA complexes, recent studies have examined the use of low molecular weight CS [8] and developed alternative methods of DNA packaging, adsorption and encapsulation [11]. It has been shown that DNA adsorbed onto the surface of CS/alginate nanoparticles (NPs) reveals a significant improvement in transfection efficiency [10]. However, surface presentation of DNA may render it susceptible to enzymatic degradation. Therefore, an ideal gene delivery system should provide an adequate protection of loaded DNA in the course of delivery and release it when appropriately.

In this study, a new approach for the enhancement of cellular uptake and transfection efficiency of CS/DNA complexes through modifying their internal structure by incorporating a negatively charged poly(γ-glutamic acid) (γ-PGA) is reported. We demonstrated that mixing CS, DNA and γ-PGA in aqueous media led to the formation of "compounded NPs" containing domains of CS/DNA and CS/γ-PGA complexes. With this unique internal structure, the compounded NPs might produce a number of even smaller CS/DNA complex NPs after disintegration within cells, thus enhancing the dissociation capacity of CS and DNA due to a large specific surface area (i.e., surface area per unit volume). γ-PGA, a naturally occurring peptide, is water-soluble, biodegradable and non-toxic. γ-PGA-based NPs have been used as a carrier for oral delivery of insulin [12,13] and been employed to deliver protein vaccines and appeared to have a great potential as an adjuvant [14].

The study was to examine characteristics of the compounded NPs containing CS, DNA and γ-PGA by dynamic light scattering (DLS), transmission electron microscopy (TEM) and small angle X-ray scattering (SAXS). The potential of gene expression and transfection efficiency of test NPs was evaluated by fluorescence and luminance spectrometry and flow cytometry, while their internalization efficiency was examined using a confocal laser scanning microscope (CLSM) and a flow cytometer.

2. Materials and Methods

2.1. Plasmid DNA

The plasmid DNAs used in the study were pEGFP-N2 (4.7 kb, coding an enhanced green fluorescence protein reporter gene, Clontech, Palo Alto, CA, USA) and pGL4.13 (4.6 kb, coding a firefly luciferase reporter gene, Promega, Madison, WI, USA). pEGFP-N2 and pGL4.13 were amplified using DH5α and purified by Qiagen Plasmid Mega Kit (Valencia, CA, USA) according to the manufacturer's instructions. The purity of plasmids was analyzed by gel electrophoresis (0.8% agarose), while their concentration was measured by UV absorption at 260 nm (Jasco, Tokyo, Japan).

2.2. Preparation of test NPs

The charge ratio (N/P/C) of test NPs was expressed as the ratio of moles of the amino groups (N) on CS to the phosphate groups (P) on DNA and the carboxyl groups (C) on γ-PGA. Test NPs at various known N/P/C molar ratios (10/1/0, 10/1/0.5, 10/1/1, 10/1/2, 10/1/4 or 10/1/6) were prepared by an ionic-gelation method. Briefly, an aqueous DNA (pEGFP-N2 or pGL4.13, 33 μg) was mixed with an aqueous γ-PGA (20 kDa, Vedan, Taichung, Taiwan) at different molar ratios (0, 0.5, 1, 2, 4 or 6) with a final volume of 100 μl. Test NPs were obtained upon addition of the mixed solution, using a pipette, into an aqueous CS (15 kDa, 0.2 μg/μl, 100 μl, pH 6.0, Challenge Bioproducts, Taichung, Taiwan) and then thoroughly mixed for 30–60 s by vortexer and left for at least 1 h at room temperature.

2.3. Characterization of test NPs

The encapsulation efficiency of DNA in each studied group was estimated by

measuring the amount of DNA left in the supernatant after centrifugation [15]. The size distribution and zeta potential of test NPs were investigated using DLS (Zetasizer 3000HS, Malvern Instruments Ltd., Worcestershire, UK). The morphology of test NPs was examined by TEM (JEOL, Tokyo, Japan) [16]. The retardation of DNA in NPs prepared at various N/P/C ratios was evaluated by electrophoresis.

The internal structure of test NPs was probed by SAXS. Aqueous suspensions of NPs were directly introduced into the sample cell comprising two ultralene windows for SAXS measurements. SAXS experiments were performed using a Bruker NanoSTAR SAXS instrument, which consisted of a Kristalloflex K760 1.5 kW X-ray generator (operated at 40 kV and 35 mA), cross-coupled Göbel mirrors for CuKα-radiation (λ = 1.54 Å) resulting in a parallel beam of about 0.05 mm^2 in cross section at the sample position and a Siemens multiwire type area detector with 1024 x 1024 resolution mode. All data were corrected by the empty beam scattering and the sensitivity of each pixel of the area detector. The area scattering pattern had been circularly averaged to increase the efficiency of data collection. The intensity profile was output as the plot of the scattering intensity (I) vs. the scattering vector, $q = 4\pi/\lambda \sin(\theta/2)$ (θ = scattering angle) [17].

The dissociation of DNA from its carrier within cells was investigated by exposing test NPs (encapsulated with pGL4.13) in a phosphate buffered saline (PBS) at pH 7.2 and then treating with restriction enzymes (*Bam*HI and *Hin*dIII, New England Biolabs, Ipswich, MA, USA), simulating the pH environments in the cytoplasms and nuclei.

2.4. In vitro transfection

HT1080 (human fibrosarcoma) cells were cultured in DMEM media supplemented with 2.2 g/l sodium bicarbonate and 10% fetal bovine serum (FBS). Cells were subcultured according to ATCC recommendations without using any antibiotic. For transfection, cells were seeded on 12-well plates at 2×10^5 cells/well and transfected the next day at 50–80% confluency. Prior to transfection, the media were removed and cells were rinsed twice with transfection media (DMEM without FBS, pH 6.0). Cells were replenished with 0.6 ml transfection media containing test NPs or naked DNA at a concentration of 2 μg DNA/well.

At 2 h post transfection, the transfection media containing NPs were removed, the cells rinsed twice with transfection media and refilled with FBS-containing media until analysis at 48 h after transfection. Cells were then observed under a fluorescence microscope (Carl Zeiss Optical, Chester, VA, USA) to monitor any morphological changes and to obtain an estimate of the transfection efficiency. Cells transfected with Lipofectamine^{TM} 2000 (Invitrogen, Carlsbad, CA, USA) were used as a positive control and those without any treatment were used as a negative control. Transfection efficiencies were presented by two numeric indicators: percentage of cells transfected and gene expression level [18].

2.5. Percentage of cells transfected

The percentage of cells transfected was quantitatively assessed at 48 h after transfection by flow cytometry. Cells were detached by 0.05% collagenase. Cell suspensions were then transferred to microtubes, fixed by 4% paraformaldehyde and determined the transfection efficiency by a flow cytometer (Beckman Coulter, Fullerton, CA, USA) equipped with a 488 nm argon laser for excitation. For each sample, 10,000 events were collected and fluorescence was detected. Signals were amplified in logarithmic mode for fluorescence to determine the EGFP positive events by a standard gating technique. The percentage of positive events was calculated as the events within the gate divided by the total number of events, excluding cell debris.

2.6. Gene expression level

The gene expression levels of cells were assayed by quantifying the expressions of EGFP or luciferase. The expression level of EGFP was quantified by comparing average fluorescence of 1×10^6 cells. Briefly, cells were treated with test NPs encapsulated with pEGFP-N2 or naked DNA. After 48 h, cells were detached as described in Section 2.5. Aliquots of 50 μl were transferred to 96-well black plates and the fluorescence intensity was analyzed using a multi-detection microplate reader (Molecular Devices, Sunnyvale, CA, USA) and normalized to the total cell number of each sample.

For the expression of luciferase, cells were plated on 24-well plates and transfected as described in Section 2.4 with the exception that 1 μg pGL4.13 was used. The cells

transfected were lysed by 100 μl of passive lysis buffer (Promega). The cell lysate was transferred into a 1.5-ml microtube, while the cell debris was separated by centrifugation (14,000 rpm, 5 min). Subsequently, a 100 μl of the luciferase assay reagent (Promega) was added to a 20 μl of the supernatant and the relative luminescence of the sample was determined by a microplate luminometer (Berthold Technologies, Bad Wildbad, Germany) and normalized to the total cell protein concentration by the Bradford method.

2.7. Fluorescent NP preparation, CLSM visualization and flow-cytometry analysis

Cy3-labeled CS (Cy3-CS) and FITC-labeled CS (FITC-CS) were synthesized as per the methods described in the literature [19,20]. To remove the unconjugated Cy3 and FITC, the synthesized Cy3-CS and FITC-CS were dialyzed in the dark against deionized (DI) water and replaced on a daily basis until no fluorescence was detected in the supernatant. The resultant Cy3-CS and FITC-CS were lyophilized in a freeze dryer. Cy3- and FITC-labeled NPs were then prepared as described in Section 2.2 to track the internalization of NPs by CLSM and to quantify their cellular uptake by flow cytometry, respectively.

To track the internalization of NPs, cells were seeded on 12-well plates with a sterile glass coverslip at 2×10^5 cells/well and incubated overnight. Subsequently, cells were rinsed twice with transfection media and transfected with Cy3-labeled NPs. After incubation for 2h, test samples were aspirated. Cells were then washed twice with pre-warmed PBS before they were fixed in 4% paraformaldehyde. Finally, the fixed cells were examined under a CLSM (TCS SL, Leica, Germany).

To quantify the cellular uptake of NPs, cells were plated on 12-well plates and transfected with FITC-labeled NPs at a concentration of 2 μg DNA/well for 1 h. After transfection, cells were detached by 0.05% collagenase and transferred to microtubes. Subsequently, cells were resuspended in PBS containing 1*mM* EDTA and fixed in 4% paraformaldehyde. Finally, the cells were introduced into a flow cytometer equipped with a 488-nm argon laser.

To determine whether cell-surface proteins were involved in the uptake of test NPs, cells were treated with trypsin (0.01%, 0.025% or 0.05% by w/v in Hanks' balanced salt

solution) for 5 min prior to transfection [21]. Cells were then treated with FITC-labeled NPs and analyzed by flow cytometry as described above.

2.8. MTT assay

The cytotoxicity of NPs was evaluated *in vitro* using the MTT assay [22]. HT1080 cells were seeded on 24-well plates at 5×10^4 cells/well, allowed to adhere overnight and transfected by test NPs containing 1 μg DNA. After 2 h, test samples were aspirated and cells were incubated for another 46 h. Subsequently, cells were incubated in a growth medium containing 1 mg/ml MTT reagent for an additional 4 h; a 500 μl of dimethyl sulfoxide was added to each well to ensure solubilization of formazan crystals. Finally, the optical density readings were performed using a multiwall scanning spectrophotometer (Dynatech Laboratories, Chantilly, VA, USA) at a wavelength of 570 nm.

2.9. Statistical analysis

Comparison between groups was analyzed by the one-tailed Student's *t*-test (SPSS, Chicago, Ill). All data are presented as a mean value with its standard deviation indicated (mean±SD). Differences were considered to be statistically significant when the *P* values were less than 0.05.

3. Results

3.1. Agarose gel retardation

The binding capacity of CS with DNA prepared at various N/P ratios was evaluated using the gel retardation assay and the results are shown in Fig. 1a. The CS/DNA complex with an N/P ratio of 5/1 was physically unstable, resulting in the partial dissociation of plasmids. In contrast, as the N/P ratio was increased to 10/1, the migration of DNA was retarded completely. Therefore, preparation of test NPs was carried out using an N/P ratio of 10/1 in the subsequent experiments. As shown in Fig. 1b, by incorporating γ-PGA in NPs (N/P/C ratios of 10/1/0.5 to 10/1/6), no significant DNA release was observed.

3.2. Morphology, size, zeta potential and encapsulation efficiency of test NPs

TEM was used to examine the morphology of test NPs prepared at various N/P/C ratios

(Fig. 2). As shown, the CS/DNA complex (N/P/C ratio of 10/1/0) had a heterogeneous size distribution with a donut, rod or pretzel shape. In contrast, with the incorporation of γ-PGA, test NPs (N/P/C ratios of 10/1/0.5 to 10/1/6) were spherical in shape with a relatively homogeneous size distribution.

The size distribution and zeta potential of the prepared NPs in aqueous environment were investigated by DLS. As shown in Table 1, with an increase in the amount of γ-PGA incorporated, the size of NPs increased appreciably while their polydispersity index and zeta potential value decreased noticeably. The diameters of NPs measured by DLS were relatively larger than those observed by TEM. This is because the diameters of NPs obtained by DLS reflected their hydrodynamic diameters swelled in aqueous solution, while those observed by TEM were the diameters of dried NPs. The encapsulation efficiencies of DNA in NPs prepared at distinct N/P/C ratios were about the same and approached 100%.

3.3. Effects of γ-PGA on internal structure of NPs and their release of DNA

SAXS was used to examine the internal structure of test NPs. Fig. 3a shows the SAXS profiles of CS/γ-PGA (N/P/C ratio of 10/0/6), CS/DNA (N/P/C ratio of 10/1/0) and CS/DNA/γ-PGA (N/P/C ratios of 10/1/1 to 10/1/6) NPs. The scattering profile of CS/γ-PGA NPs displayed a featureless monotonic decay, revealing a disordered internal structure. In this case, the SAXS intensity might stem from the characteristic concentration fluctuations of the CS/γ-PGA complex within NPs. The SAXS profile of CS/DNA NPs was found to display a peak at 2.8 nm^{-1} associated with the spatial correlation of DNA in CS/DNA complexes. The characteristic spacing between DNA calculated from the peak position (q_{DNA}) *via* $d_{DNA} = 2\pi/q_{DNA}$ was 2.24 nm. Therefore, the DNA chains in CS/DNA complexes were packed densely to form a tight bundle phase, as the positively charged CS chains wrapped around DNA for charge matching caused a significant aggregation of DNA.

The DNA correlation peak associated with CS/DNA complexes was also observable in the SAXS profiles of NPs containing CS, DNA and γ-PGA. Interestingly, this peak was located at a higher q (3.0 nm^{-1}) than that associated with the binary CS/DNA complex,

showing that the incorporation of γ-PGA induced a more compact packing of DNA chains (with a reduction of d_{DNA} to 2.10 nm). Moreover, an excess intensity (marked by the arrow in Fig. 3a) was identified at lower q for the ternary system (CS/DNA/γ-PGA) and it became more significant at a higher content of γ-PGA. The presence of this intensity contribution implied the existence of a heterogeneity or domains with a characteristic length scale larger than d_{DNA} in NPs.

The features of SAXS patterns indicated that the NPs formed by the ternary system were composed of two types of domains containing CS/DNA and CS/γ-PGA complexes, as schematically illustrated in Fig. 3b. This type of NPs is called "compounded NPs" here. The dense packing of DNA chains in CS/DNA domains gave rise to the scattering peak, while the CS/γ-PGA domains surrounding the CS/DNA domains contributed to the excess intensity observed at lower q. In this case, the CS/γ-PGA domains might create a relatively rigid environment to suppress the positional distortion of the DNA chains induced by thermal fluctuations; as a result, the DNA chains in CS/DNA domains exhibited a more compact packing. In addition, we expected the presence of unbounded (or pendant) segments of CS chains emanating from the surface of CS/γ-PGA complexes; these pendant CS segments might subsequently bridge with the neighboring DNA chains to from two types of domains containing CS/γ-PGA and CS/DNA complexes within the compounded NPs (Fig. 3b).

After being exposed at pH 7.2 and subsequently treated by restriction enzymes (*Bam*HI and *Hin*dIII), simulating the environments in the cytoplasms and nuclei, test NPs were analyzed by gel electrophoresis. As shown in Fig. 3c, there were three DNA bands (4.6, 2.7 and 1.9 kb, respectively, digested by restriction enzymes) identified in gel for each studied group. With increasing the amount of γ-PGA incorporated in NPs, the intensities of DNA bands observed in gel were stronger. These results implied that incorporation of polyanionic γ-PGA might enhance the release of DNA from NPs within cells (i.e., at pH ~7.2).

3.4. Percentage of cells transfected and gene expression level

To determine the percentage of cells that actually expressed the transgene, we counted the number of EGFP-positive cells using flow cytometry at 48 h post transfection. As shown in Fig. 4a, only up to 15% of the cells produced EGFP when transfected with the NPs containing no γ-PGA (N/P/C ratio of 10/1/0, i.e., CS/DNA NPs). By incorporating γ-PGA in NPs (N/P/C ratios of 10/1/0.5 to 10/1/6), a significant increase in the percentage of cells that expressed EGFP was found. Transfection was increased approximately 4-fold (55%) for the cells transfected with the NPs with an N/P/C ratio of 10/1/4 compared to those treated with the NPs containing no γ-PGA ($P < 0.05$).

The results of expression levels of EGFP or luciferase of cells are given in Fig. 4b and 4c, respectively. As shown, the EGFP expression levels of cells transfected with the NPs incorporating γ-PGA were significantly higher than those treated with the NPs containing no γ-PGA ($P < 0.05$). The luciferase gene expression of cells transfected by the NPs with an N/P/C ratio of 10/1/4 was about 10-fold increased in comparison with those treated with the NPs containing no γ-PGA ($P < 0.05$). These results indicated that the transfection efficiency of NPs was significantly enhanced after the incorporation of γ-PGA. Among all studied groups, the cells transfected with the NPs with an N/P/C ratio of 10/1/4 had the highest gene expression level.

3.5. Cellular uptake

CLSM was used to visualize the cellular uptake of Cy3-labeled NPs and their EGFP expression. The results of fluorescence images of cells after exposure to NPs prepared at different N/P/C ratios are shown in Fig. 5a and 5b. At 2 h after transfection, accumulation of Cy3-lableded NPs was observed in most of the incubated cells in all studied groups (Fig. 5a). The fluorescence intensity observed in cells increased notably with increasing the amount of γ-PGA incorporated in NPs. At this time, no EGFP expression was observed for all of the studied groups. At 48 h after transfection, it appeared that the numbers of cells that expressed EGFP in the groups transfected with the NPs incorporating γ-PGA were more than the group treated with the NPs containing no γ-PGA (Fig. 5b).

After a 2-h transfection, the percentage of cells that internalized FITC-labeled NPs and their fluorescence intensity were quantified by flow cytometry. As shown in Fig. 5c and 5d, the percentage of fluorescent cells and their fluorescence intensity upon internalization of NPs were significantly enhanced with increasing the amount of γ-PGA incorporated ($P < 0.05$). However, there were no statistically significant differences between test NPs with N/P/C ratios of 10/1/4 and 10/1/6 ($P > 0.05$).

To further elucidate differences in the uptake mechanism, the interaction of NPs with cell membranes was investigated by treating cells with trypsin at different concentrations prior to transfection. As shown in Fig. 6a, trypsinization resulted in a significant decrease in the internalization of FITC-labeled NPs with or without γ-PGA ($P < 0.05$). However, trypsin did not induce a concentration-dependent effect on the uptake of the NPs containing no γ-PGA (Fig. 6a and 6b, $P > 0.05$), while it caused a concentration-dependent decrease in the internalization of the NPs incorporating γ-PGA (Fig. 6a and 6c, $P < 0.05$). These results implied that by incorporating γ-PGA, test NPs might be internalized by cells via a specific protein-mediated endocytosis.

3.6. MTT assay

Fig. 7 shows the viability of cells cultured in the media treated with varying test samples. As shown, the cytotoxicity of naked DNA, γ-PGA and CS was quite low. The viability of the cells treated with test NPs decreased relatively with increasing the amount of γ-PGA incorporated.

4. Discussion

CS/DNA complex NPs have been considered as a candidate for gene delivery [23–24]. Although advantageous for DNA packing and protection, CS-based complexes may lead to difficulties in DNA release once they arrive at the site of action [11], thus limiting their transfection efficiency. In the study, we demonstrated that after the incorporation of γ-PGA in CS/DNA NPs, the percentage of cells transfected and their gene expression level were significantly enhanced (Fig. 4a–4c and 5b).

The p*K*a values of CS and γ-PGA are 6.5 and 2.9, respectively [25]. When prepared in DI water (pH 6.0), CS, DNA and γ-PGA are ionized. The ionized CS, DNA and γ-PGA can form polyelectrolyte complexes (CS/DNA/γ-PGA NPs) by electrostatic interactions between the positively charged amino groups ($-NH_3^+$) on CS and the negatively charged phosphate groups ($-PO_4^-$) on DNA and carboxyl groups ($-COO^-$) on γ-PGA.

The SAXS results revealed that DNA and γ-PGA formed complexes with CS separately to yield two types of domains bridged by pendant CS chains in the compounded NPs (Fig. 3b) [9,26]. After internalization into cells, the compounded NPs would be expected to disintegrate into a number of even smaller sub-particles composing CS/DNA and CS/γ-PGA complexes, due to deprotonation of the bridged CS chains. The subsequent release of DNA through the disruption of these sub-particles became relatively easier than that from the larger CS/DNA NPs prepared without adding γ-PGA, because of their significantly greater specific surface area. Therefore, the compounded NPs prepared by incorporating γ-PGA not only offered a protection of loaded DNA in the course of delivery but also enhanced the release of DNA within cells [24].

However, as the amount of γ-PGA incorporated was increased to a critical value, the transfection efficiency of CS/DNA/γ-PGA NPs (N/P/C ratio of 10/1/6) started to drop appreciably (Fig. 4a and 4b). When beyond this threshold, there might be too many dissociated DNA molecules exposed to cytosolic nuclease(s), thus leading to their degradation before entry of the nucleus [27]. As indicated in Fig. 3c, with increasing the amount of γ-PGA incorporated in CS/DNA/γ-PGA NPs, DNA was more susceptible to enzymatic degradation in the environments simulating the cytoplasms and nuclei.

Interestingly, in addition to improving the release of DNA intracellularly, the incorporation of γ-PGA in test NPs significantly enhanced their cellular internalization (Fig. 5a, 5c and 5d). Cellular entry can be realized by distinct mechanisms that may lead to disparate percentages of cellular uptake and therefore different transfection efficiencies [28]. It is known that a number of polyplexes can induce cellular internalization through a non-specific charge-mediated interaction with proteoglycans that are present on cell

membranes [29]. These highly anionic proteoglycans determine much of the interactions between the cell surface and extracellular macromolecules [30] and believed to play an important role in the cellular uptake of many non-targeted, positively charged gene delivery vectors [29,31].

Trypsinization resulted in a substantial reduction in surface-bound proteins on the cell surface. As shown in Fig. 6a and 6b, after trypsinization, a remarkable decrease in the percentage of cellular uptake of CS/DNA NPs was observed; however, this phenomenon was in a trypsin concentration-independent manner. These results implied that the internalization of CS/DNA NPs might be mainly via a non-specific charge-mediated interaction between the NPs (positively charged) and the components of cell membranes (negatively charged proteoglycans, Fig. 8a) [11].

In contrast, a trypsin concentration-dependent reduction of the cellular uptake of CS/DNA/γ-PGA NPs was observed (Fig. 6a and 6c). This observation suggested that besides a non-specific charged-mediated binding to cell membranes, there were specific trypsin-cleavable proteins involved in the internalization of CS/DNA/γ-PGA NPs (Fig. 8b), indicating that γ-PGA played a crucial role in the cellular uptake of CS/DNA/γ-PGA NPs. This might explain why there was a significantly more cellular internalization of CS/DNA/γ-PGA NPs than their CS/DNA counterparts (Fig. 5a, 5c and 5d). However, the exact mechanism by which these specific membrane-present proteins mediate the cellular uptake of CS/DNA/γ-PGA NPs remains to be understood.

5. Conclusions

A new CS-based NP system incorporating γ-PGA was developed in the study as an efficient vector for gene delivery. The analysis of our SAXS results indicated that incorporating γ-PGA would cause the formation of compounded NPs whose internal structure might facilitate the dissociation of CS and DNA. In addition to improving the release of DNA intracellularly, the incorporation of γ-PGA in NPs markedly increased their cellular internalization. Taken together, γ-PGA significantly enhanced the transfection

efficiency of this newly developed gene-delivery system.

Acknowledgments

This work was supported by a grant from the National Science Council (NSC97-2120-M-007-001), Taiwan, Republic of China. The synchrotron X-ray scattering experiment supported by the NSRRC under Project ID 2007-1-018-4 was gratefully acknowledged.

References

[1] Jin J, Song M, Hourston DJ. Novel chitosan-based films cross-linked by genipin with improved physical properties. Biomacromolecules 2004;5:162-8.

[2] Iwasaki N, Yamane ST, Majima T, Kasahara Y, Minami A, Harada K, et al. Feasibility of polysaccharide hybrid materials for scaffolds in cartilage tissue engineering: evaluation of chondrocyte adhesion to polyionic complex fibers prepared from alginate and chitosan. Biomacromolecules 2004;5:828-33.

[3] Mao HQ, Roy K, Troung-Le VL, Janes KA, Lin KY, Wang Y, et al. Chitosan-DNA nanoparticles as gene carriers: synthesis, characterization and transfection efficiency. J Controlled Release 2001;70:399-421.

[4] Kim TH, Park IK, Nah JW, Choi YJ, Cho CS. Galactosylated chitosan/DNA nanoparticles prepared using water-soluble chitosan as a gene carrier. Biomaterials 2004;25: 3783-92.

[5] Morille M, Passirani C, Vonarbourg A, Clavreul A, Benoit JP. Progress in developing cationic vectors for non-viral systemic gene therapy against cancer. Biomaterials 2008; 29:3477-96.

[6] Kim TH, Jiang HL, Jere D, Park IK, Cho MH, Nah JW, et al. Chemical modification of chitosan as a gene carrier in vitro and in vivo. Prog Polym Sci 2007;32:726-53.

[7] Lee MK, Chun SK, Choi WJ, Kim JK, Choi SH, Kim A, et al. The use of chitosan as a condensing agent to enhance emulsion-mediated gene transfer. Biomaterials 2005; 26:2147-56.

[8] Lavertu M, Méthot S, Tran-Khanh N, Buschmann MD. High efficiency gene transfer using chitosan/DNA nanoparticles with specific combinations of molecular weight and degree of deacetylation. Biomaterials 2006;27:4815-24.

[9] Lee PW, Peng SF, Su CJ, Mi FL, Chen HL, Wei MC, et al. The use of biodegradable polymeric nanoparticles in combination with a low-pressure gene gun for transdermal DNA delivery. Biomaterials 2008;29:742-51.

[10] Douglas KL, Piccirillo CA, Tabrizian M. Effects of alginate inclusion on the vector

properties of chitosan-based nanoparticles. J Controlled Release 2006;115:354-61.

[11] Wong SY, Pelet J, Putnam D. Polymer systems for gene delivery—Past, present, and future. Prog Polym Sci 2007;32:799-837.

[12] Lin YH, Mi FL, Chen CT, Chang WC, Peng SF, Liang HF, et al. Preparation and characterization of nanoparticles shelled with chitosan for oral insulin delivery. Biomacromolecules 2007;8:146-52.

[13] Mi FL, Wu YY, Lin YH, Sonaje K, Ho YC, Chen CT, et al. Oral delivery of peptide drugs using nanoparticles self-assembled by poly(gamma-glutamic acid) and a chitosan derivative functionalized by trimethylation. Bioconjug Chem 2008;19:1248-55.

[14] Wang X, Uto T, Akagi T, Akashi M, Baba M. Poly(gamma-glutamic acid) nanoparticles as an efficient antigen delivery and adjuvant system: potential for an AIDS vaccine. J Med Virol 2008;80:11-9.

[15] Cui Z, Mumper RJ. Chitosan-based nanoparticles for topical genetic immunization. J Controlled Release 2001;75:409-19.

[16] Adams CWM. Osmium tetroxide and the marchi method: reactions with polar and non-polar lipids, protein and polysaccharide. J Histochem Cytochem 1960;8:262-7.

[17] Hsu WL, Li YC, Chen HL, Liou W, Jeng US, Lin HK, et al. Thermally-induced order-order transition of DNA-cationic surfactant complexes. Langmuir 2006;22:7521-7.

[18] Ko IK, Ziady A, Lu S, Kwon YJ. Acid-degradable cationic methacrylamide polymerized in the presence of plasmid DNA as tunable non-viral gene carrier. Biomaterials 2008:29:3872-81.

[19] Qaqish RB, Amiji MM. Synthesis of a fluorescent chitosan derivative and its application for the study of chitosan-mucin interactions. Carbohydr Polym 1999;38:99-107.

[20] Ho YP, Chen HH, Leong KW, Wang TH. Evaluating the intracellular stability and unpacking of DNA nanocomplexes by quantum dots-FRET. J Controlled Release 2006;116:83-9.

[21] Szolnoky G, Bata-Csörgö Z, Kenderessy AS, Kiss M, Pivarcsi A, Novák Z, et al. A mannose-binding receptor is expressed on human keratinocytes and mediates killing of *Candida albicans*. J Invest Dermatol 2001;117:205-13.

[22] Liang HF, Yang TF, Huang CT, Chen MC, Sung HW. Preparation of nanoparticles composed of poly(gamma-glutamic acid)-poly(lactide) block copolymers and evaluation of their uptake by HepG2 cells. J Controlled Release 2005;105:213-25.

[23] Dang JM, Leong KW. Natural polymers for gene delivery and tissue engineering. Adv Drug Deliv Rev 2006;58:487-99.

[24] Kiang T, Wen J, Lim HW, Leong KW. The effect of the degree of chitosan deacetylation on the efficiency of gene transfection. Biomaterials 2004;25:5293-301.

[25] Lin YH, Chen CT, Liang HF, Kulkarni AR, Lee PW, Chen CH, et al. Novel nanoparticles for oral insulin delivery via the paracellular pathway. Nanotechnology 2007;18:105102.

[26] DeRouchey J, Netz RR, Rädler JO. Structural investigations of DNA-polycation complexes. Eur Phys J E Soft Matter 2005;16:17-28.

[27] Lechardeur D, Sohn KJ, Haardt M, Joshi PB, Monck M, Graham RW, et al. Metabolic instability of plasmid DNA in the cytosol: a potential barrier to gene transfer. Gene Ther 1999;6:482-97.

[28] Douglas KL, Piccirillo CA, Tabrizian M. Cell line-dependent internalization pathways and intracellular trafficking determine transfection efficiency of nanoparticle vectors. Eur J Pharm Biopharm 2008;68:676-87.

[29] Mislick KA, Baldeschwieler JD. 1996. Evidence for the role of proteoglycans in cation-mediated gene transfer. Proc Natl Acad Sci U S A 1996;93:12349-54.

[30] Yanagishita M, Hascall VC. Cell surface heparan sulfate proteoglycans. J Biol Chem 1992;267:9451-4.

[31] Kichler A, Mason AJ, Bechinger B. Cationic amphipathic histidine-rich peptides for gene delivery. Biochim Biophys Acta 2006;1758:301-7.

Figure Captions

Figure 1. (a) Gel retardation analyses of CS/DNA complex nanoparticles prepared at different N/P ratios. Samples were run on a 0.8% agarose gel and subsequently stained using ethidium bromide. Complete complexation of DNA was noted at an N/P ration of 10/1; (b) Gel retardation analyses of CS/DNA/γ-PGA nanoparticles prepared at different N/P/C ratios.

Figure 2. TEM micrographs of CS/DNA/γ-PGA nanoparticles prepared at different N/P/C ratios.

Figure 3. (a) SAXS profiles of CS/γ-PGA, CS/DNA and CS/DNA/γ-PGA complex nanoparticles. The arrow marks the excess intensity arising from the CS/γ-PGA domains in complexes formed in the ternary system (CS/DNA/γ-PGA nanoparticles); (b) Schematic illustrations of the internal structures of CS/DNA and CS/DNA/γ-PGA complex nanoparticles; (c) Agarose gel electrophoresis of the DNA released from CS/DNA/γ-PGA nanoparticles prepared at different N/P/C ratios. Prior to electrophoresis, test nanoparticles were exposed in a phosphate buffered saline at pH 7.2 and then treated with restriction enzymes [*Bam*HI (B) and *Hin*dIII (H)], simulating the pH environments in the cytoplasms and nuclei.

Figure 4. Efficiencies of cell transfection: (a) percentages of cells that were transfected; (b) relative fluorescence intensities of transfected cells that expressed EGFP protein; (c) normalized luciferase activities of transfected cells that expressed the luciferase. Cells were transfected *in vitro* using CS/DNA/γ-PGA nanoparticles prepared at different N/P/C ratios (n = 5). NC: negative control (the group without any treatment); NK: naked DNA; LF: Lipofectamine^{TM} 2000.

Figure 5. (a) Confocal images of cells transfected with Cy3-labeled CS/DNA/γ-PGA nanoparticles prepared at different N/P/C ratios for 2 h; (b) EGFP expressions of cells transfected with Cy3-labeled CS/DNA/γ-PGA nanoparticles prepared at different N/P/C ratios for 48 h; (c) Percentages of cellular uptake of FITC-labeled CS/DNA/γ-PGA nanoparticles prepared at different N/P/C ratios, analyzed by flow

cytometry (n = 3); (d) Intracellular fluorescence intensities of CS/DNA/γ-PGA nanoparticles prepared at different N/P/C ratios determined by flow cytometry. NC: negative control (the group without any treatment).

Figure 6. Results of intracellular uptake of CS/DNA and CS/DNA/γ-PGA (N/P/C ratio of 10/1/4) nanoparticles after the cells being treated with different concentrations of trypsin, determined by flow cytometry: (a) percentages of intracellular uptake of test nanoparticles (n = 3); (b) fluorescence intensities after intracellular uptake of CS/DNA nanoparticles; (c) fluorescence intensities after intracellular uptake of CS/DNA/γ-PGA nanoparticles.

Figure 7. Results of the cell viability after being treated with CS/DNA/γ-PGA nanoparticles prepared at different N/P/C ratios determined by the MTT assay (n = 5). NC: negative control (the group without any treatment); NK: naked DNA; γ-PGA: poly(γ-glutamic acid); CS: chitosan; LF: Lipofectamine^{TM} 2000.

Figure 8. Schematic illustrations of potential uptake pathways: (a) CS/DNA nanoparticles. The internalization of CS/DNA nanoparticles might be mainly via a non-specific charge-mediated interaction between the nanoparticles (positively charged) and the components of cell membranes (negatively charged proteoglycans); (b) CS/DNA/γ-PGA nanoparticles. Besides a non-specific charged-mediated binding to cell membranes, there were specific trypsin-cleavable proteins involved in the internalization of CS/DNA/γ-PGA nanoparticles.

Table

Table 1. Size, polydispersity index (PI), zeta potential and encapsulation efficiency (EE) of pEGFP-N2 of test nanoparticles prepared at distinct N/P/C ratios (n = 5).

N/P/C Ratio	Size (nm)	PI	Zeta Potential (mV)	EE (%)
N/P/C=10/1/0	140.2±7.7	0.33±0.04	31.7±0.8	97.7±0.4
N/P/C=10/1/0.5	135.5±3.2	0.21±0.01	35.3±0.3	97.3±0.9
N/P/C=10/1/1	130.8±1.3	0.20±0.01	34.5±0.2	96.1±0.6
N/P/C=10/1/2	132.8±4.9	0.22±0.03	33.3±1.1	94.2±0.4
N/P/C=10/1/4	152.5±5.1	0.16±0.02	28.7±1.2	99.5±0.1
N/P/C=10/1/6	204.5±3.7	0.11±0.01	18.7±0.2	99.5±0.1

Figure 1

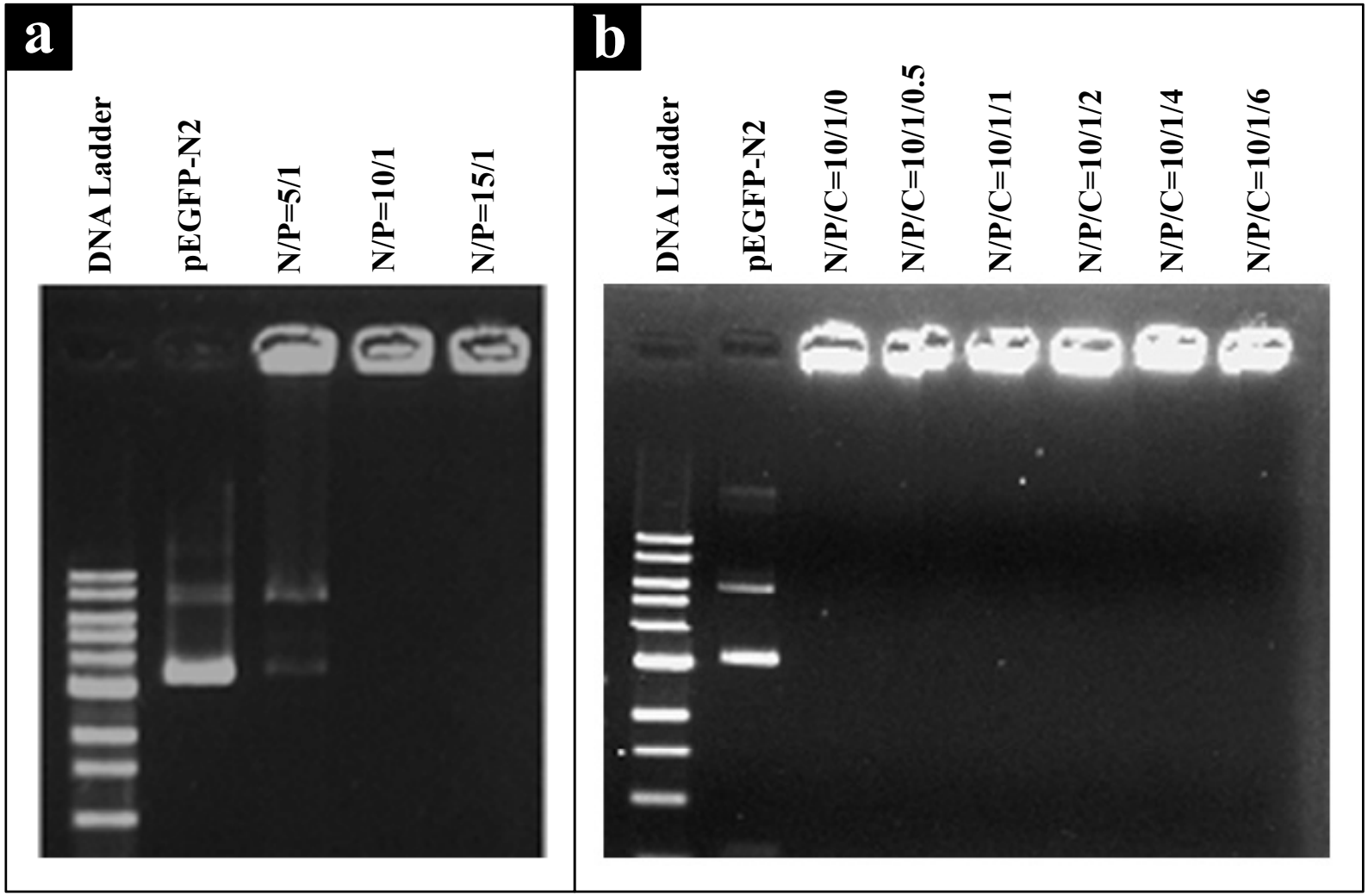
a
DNA Ladder
pEGFP-N2
N/P=5/1
N/P=10/1
N/P=15/1
b
DNA Ladder
pEGFP-N2
N/P/C=10/1/0
N/P/C=10/1/0.5
N/P/C=10/1/1
N/P/C=10/1/2
N/P/C=10/1/4
N/P/C=10/1/6

Figure 2

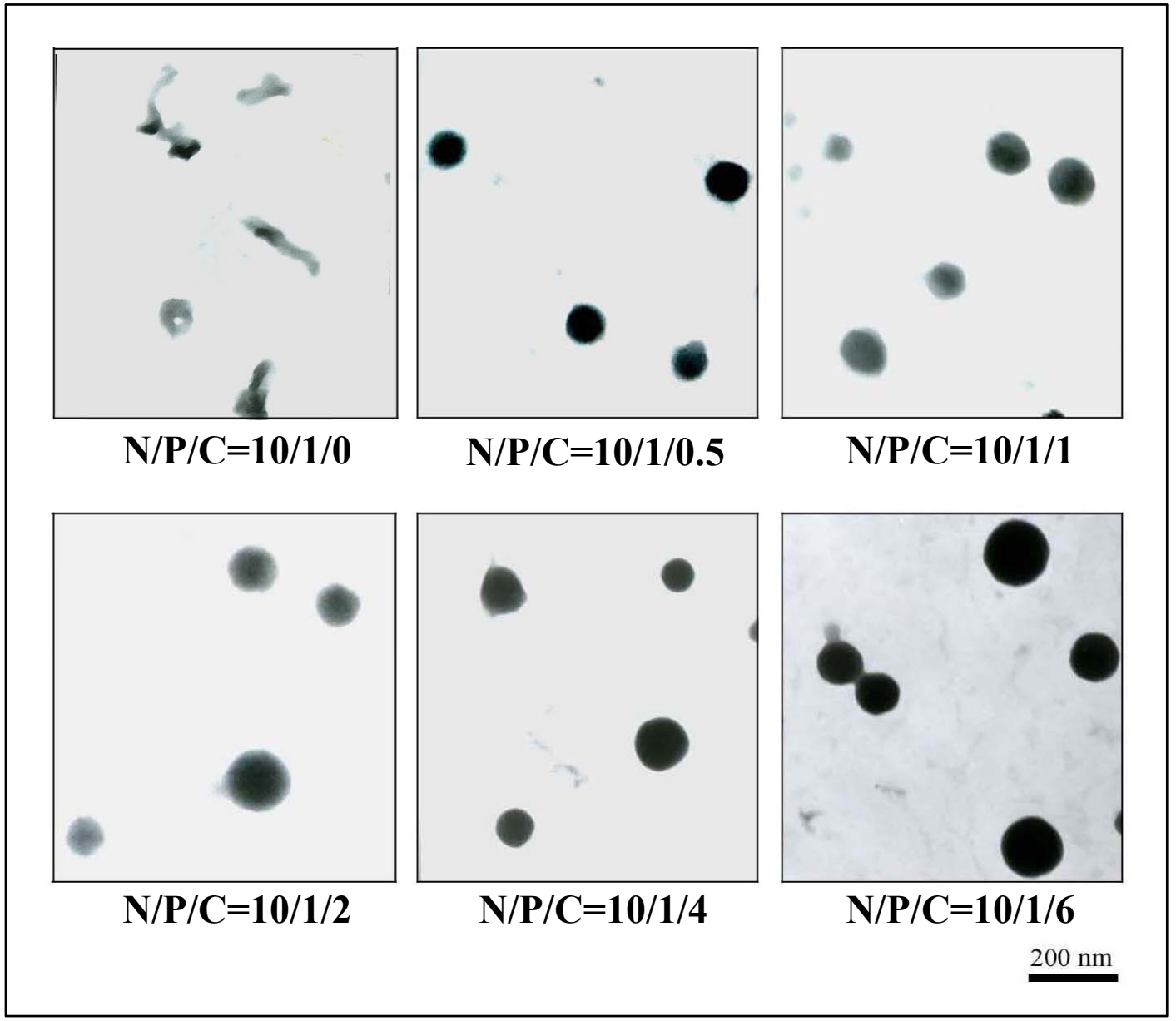

Figure 3a

Figure 3

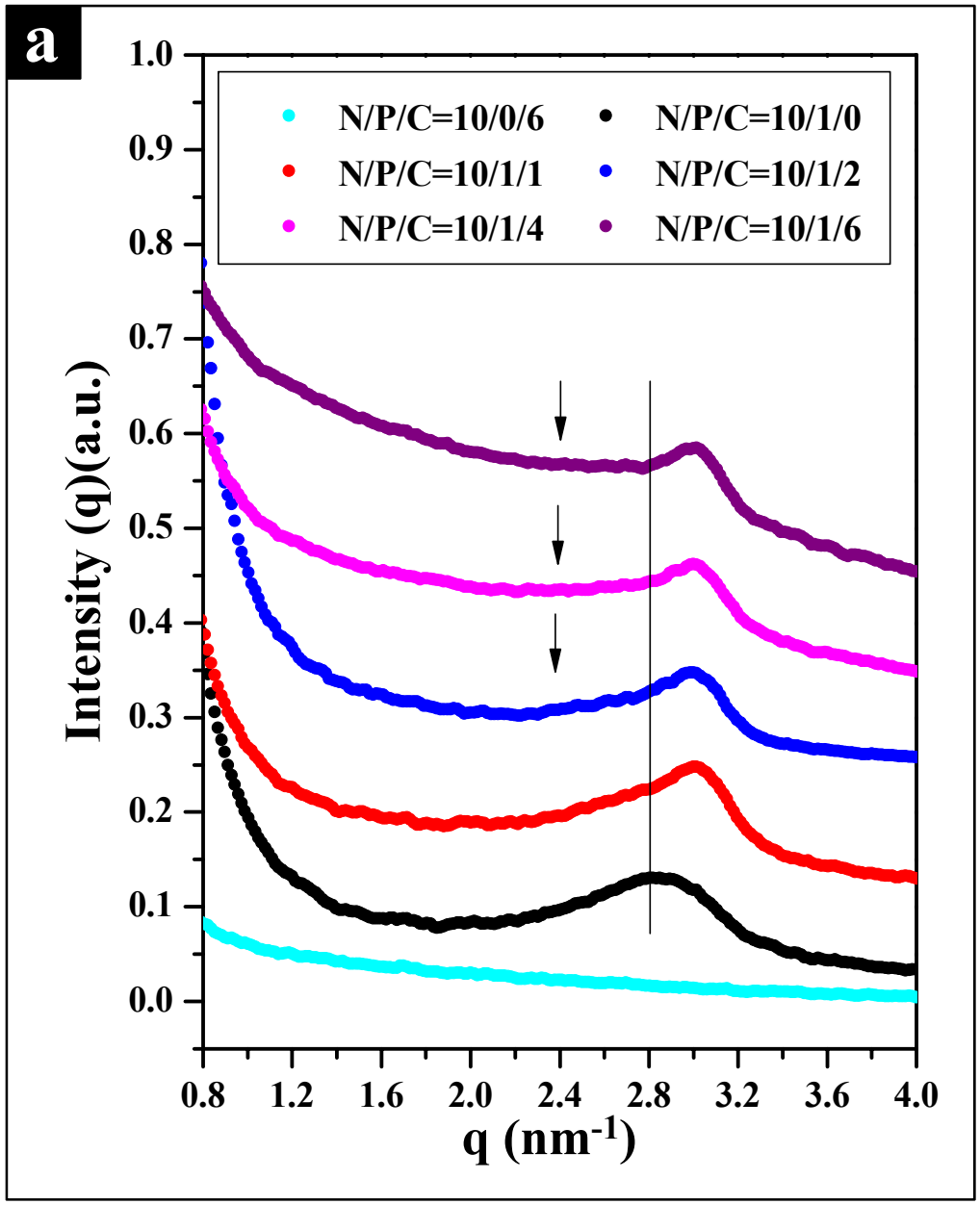

Figure3b

Figure 3

b

CS/DNA Complexes

CS/DNA Domain

d_{DNA}=2.24 nm

CS/DNA Domain

Shortly after Endocytosis

Deprotonation of CS Chains

CS/DNA/ γ -PGA Complexes (Compounded NPs)

CS/DNA and CS/ γ -PGA Domains Bridged by Pendant CS Chains

d_{DNA}=2.10 nm

CS/DNA Domain

CS/ γ -PGA Domain

Deprotonation of Bridged CS Chains

Dissociation of CS/DNA and CS/ γ -PGA Domains

or DNA

CS

γ -PGA

Figure 3c

Figure 3

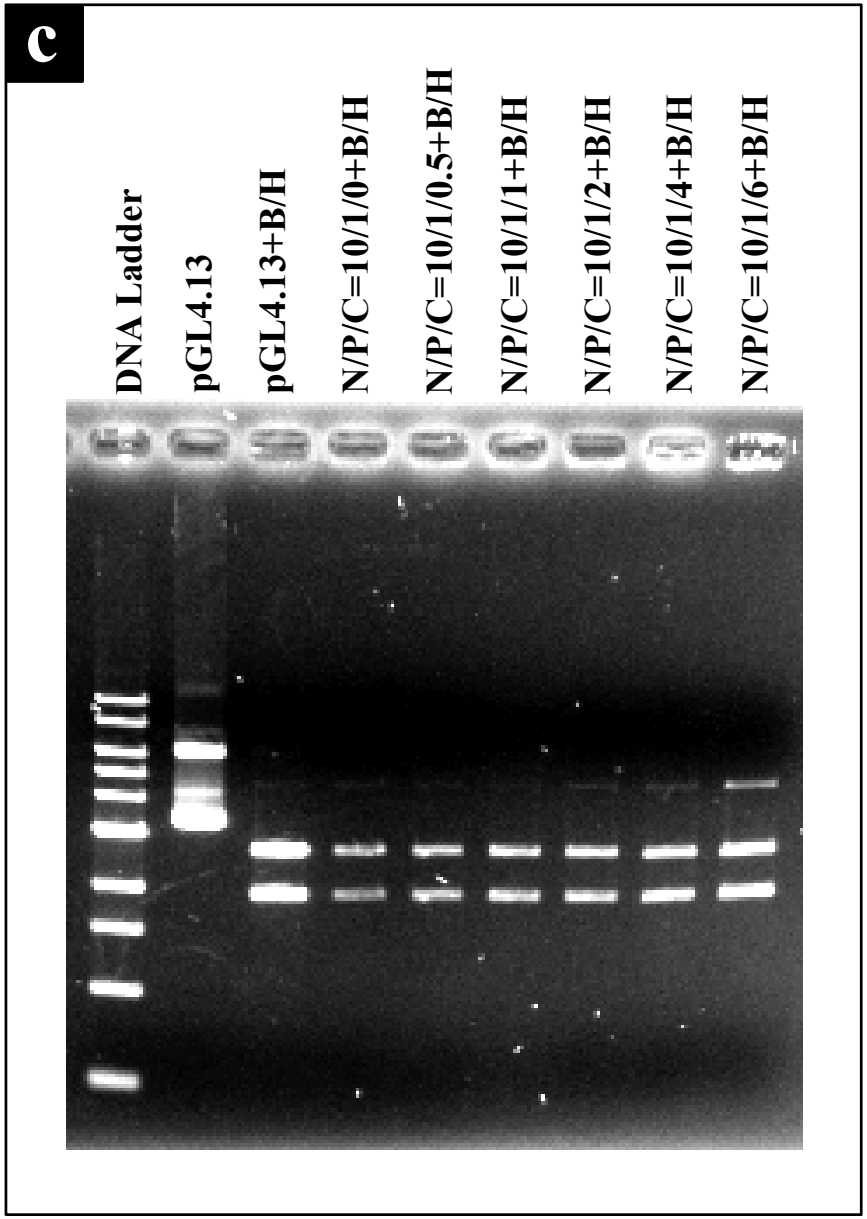

Figure 4a

Figure 4

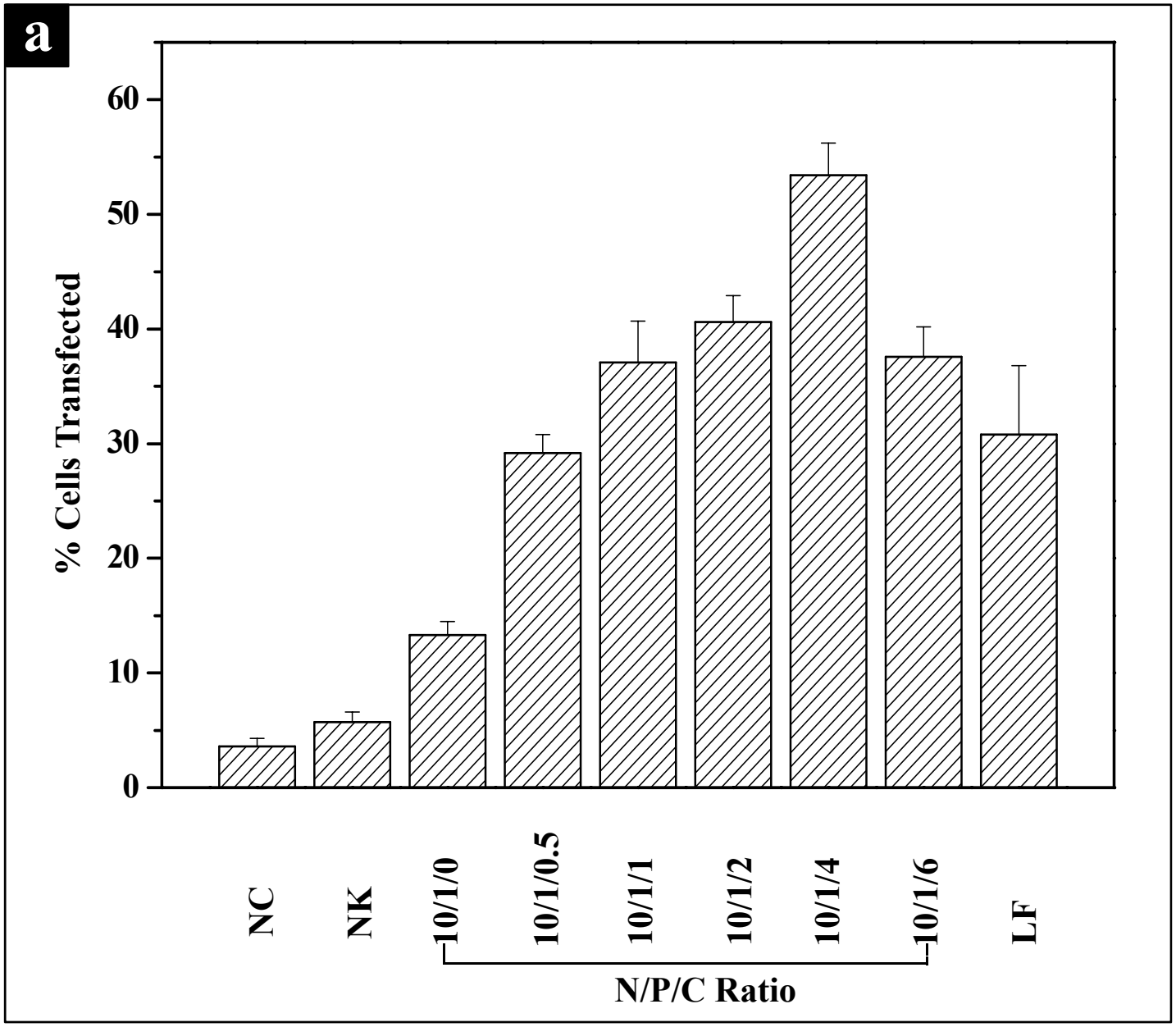

Figure 4b

Figure 4

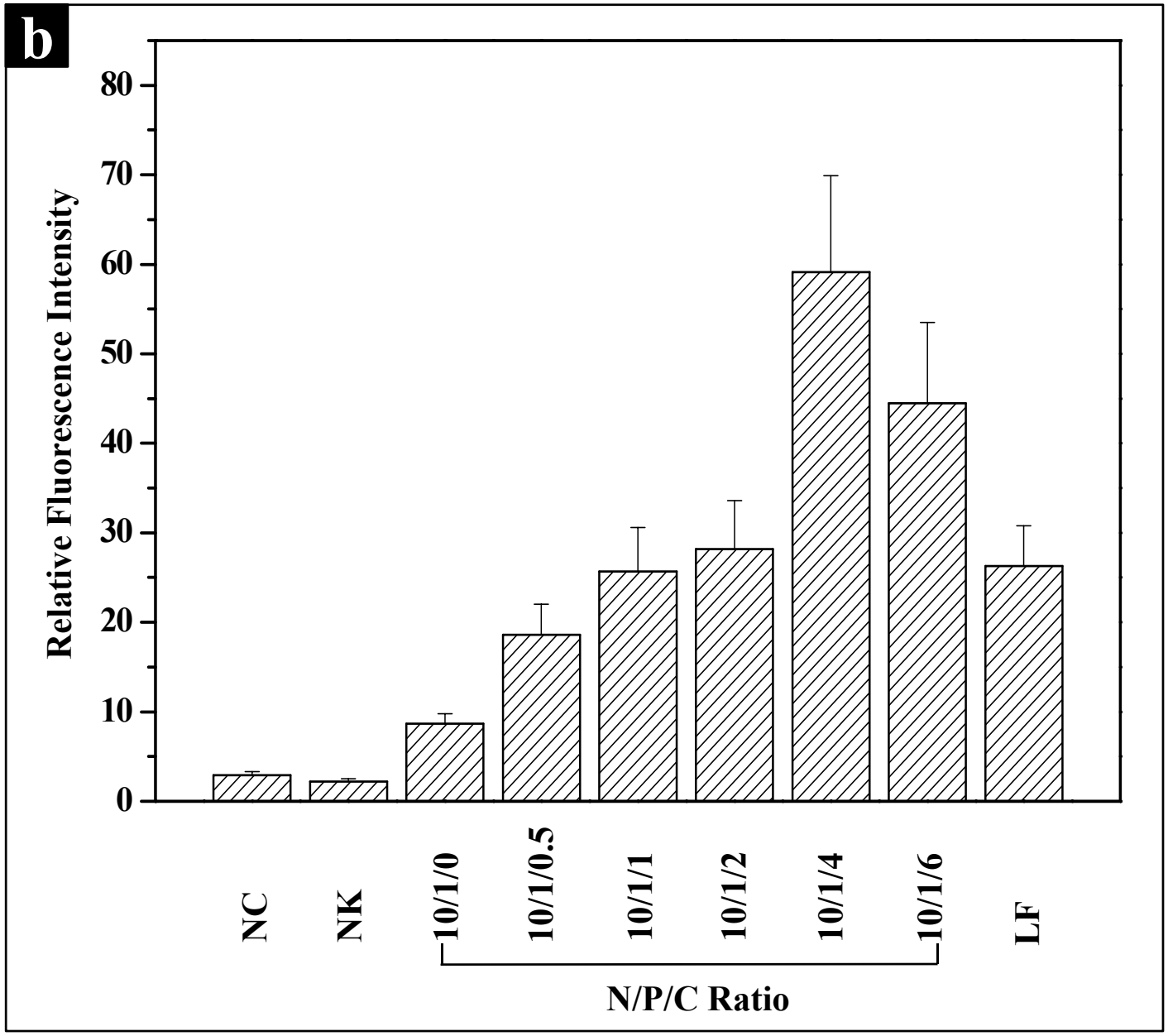

Figure 4c

Figure 4

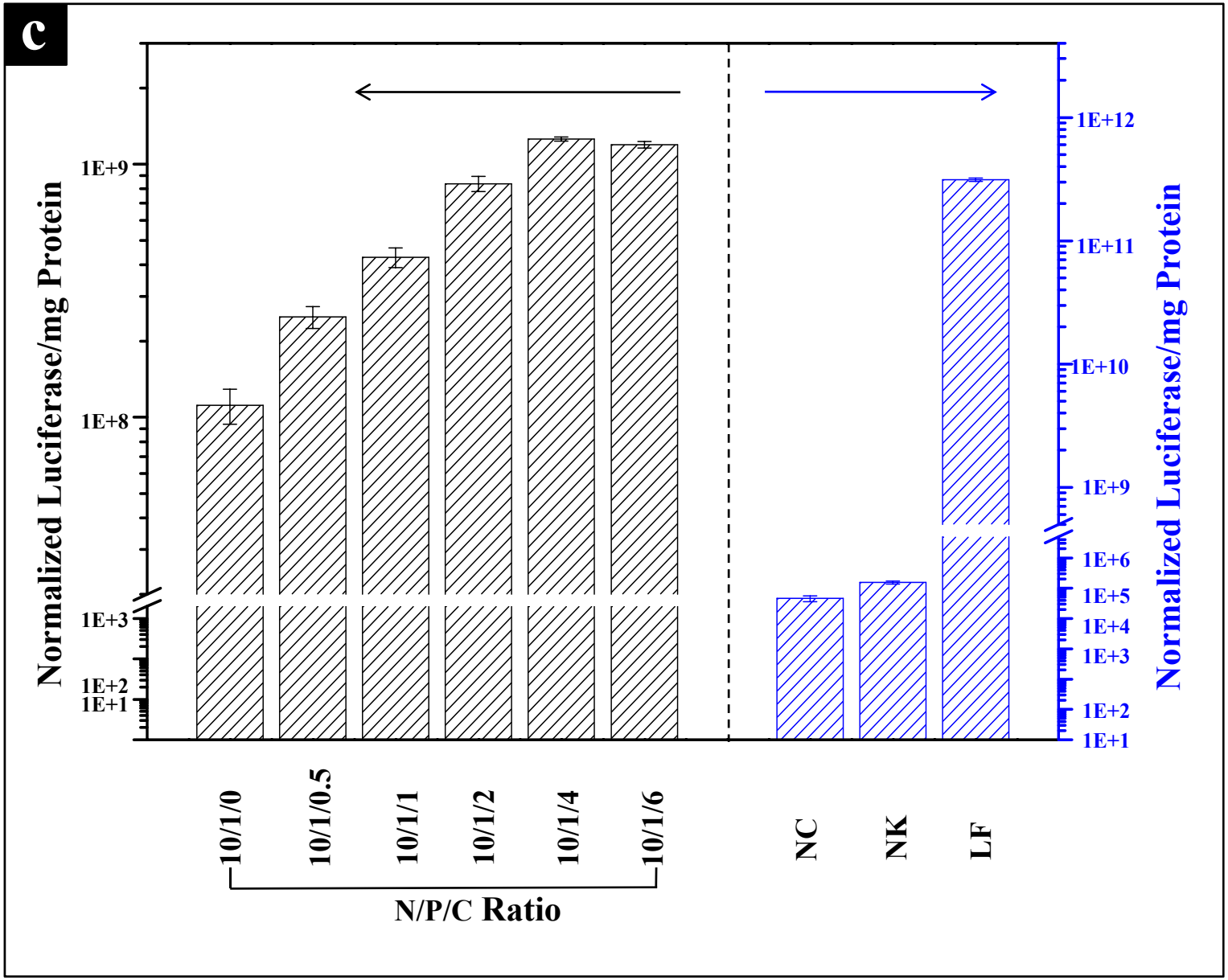

Figure 5a

Figure 5

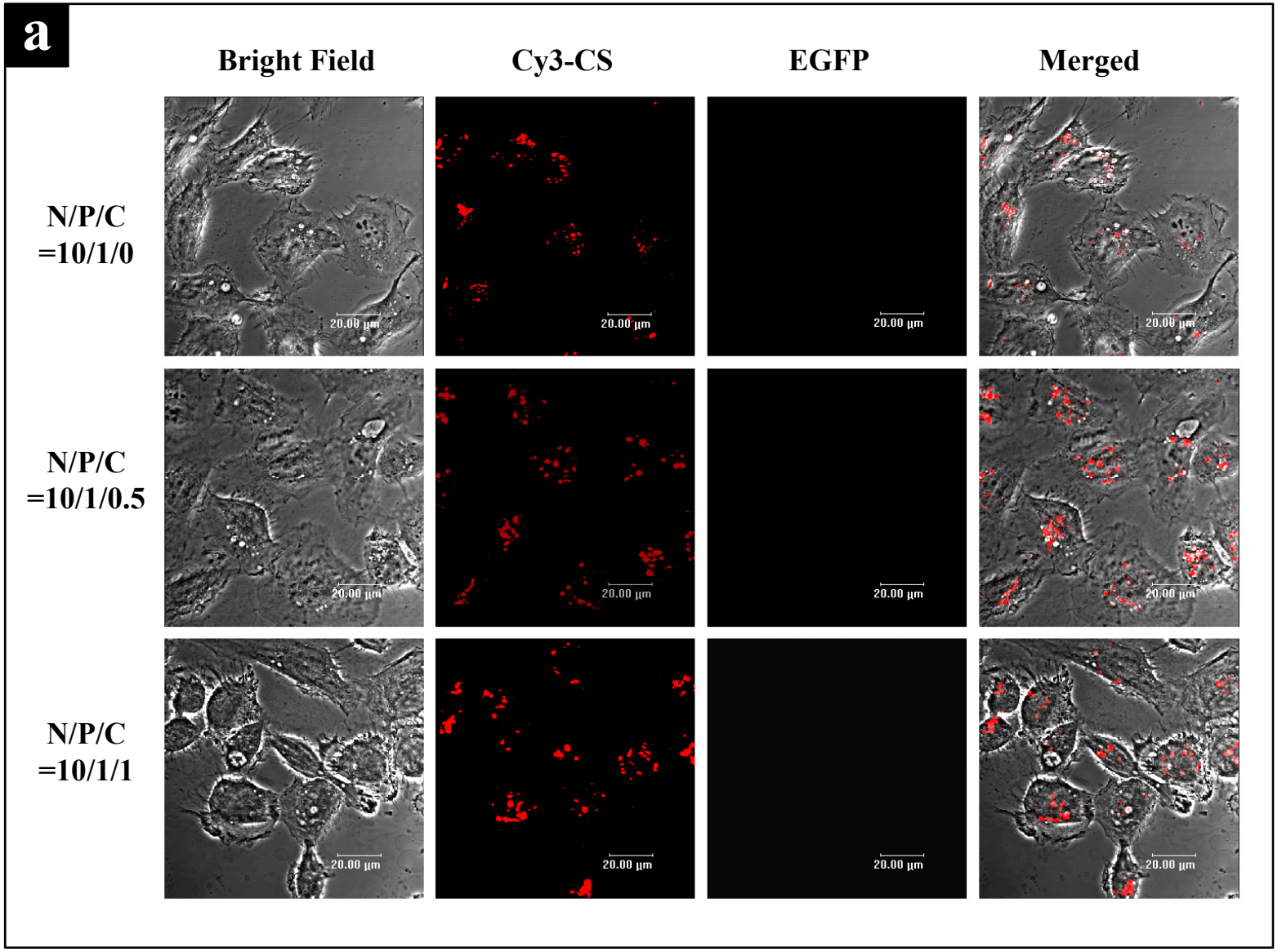

Figure 5 Continued

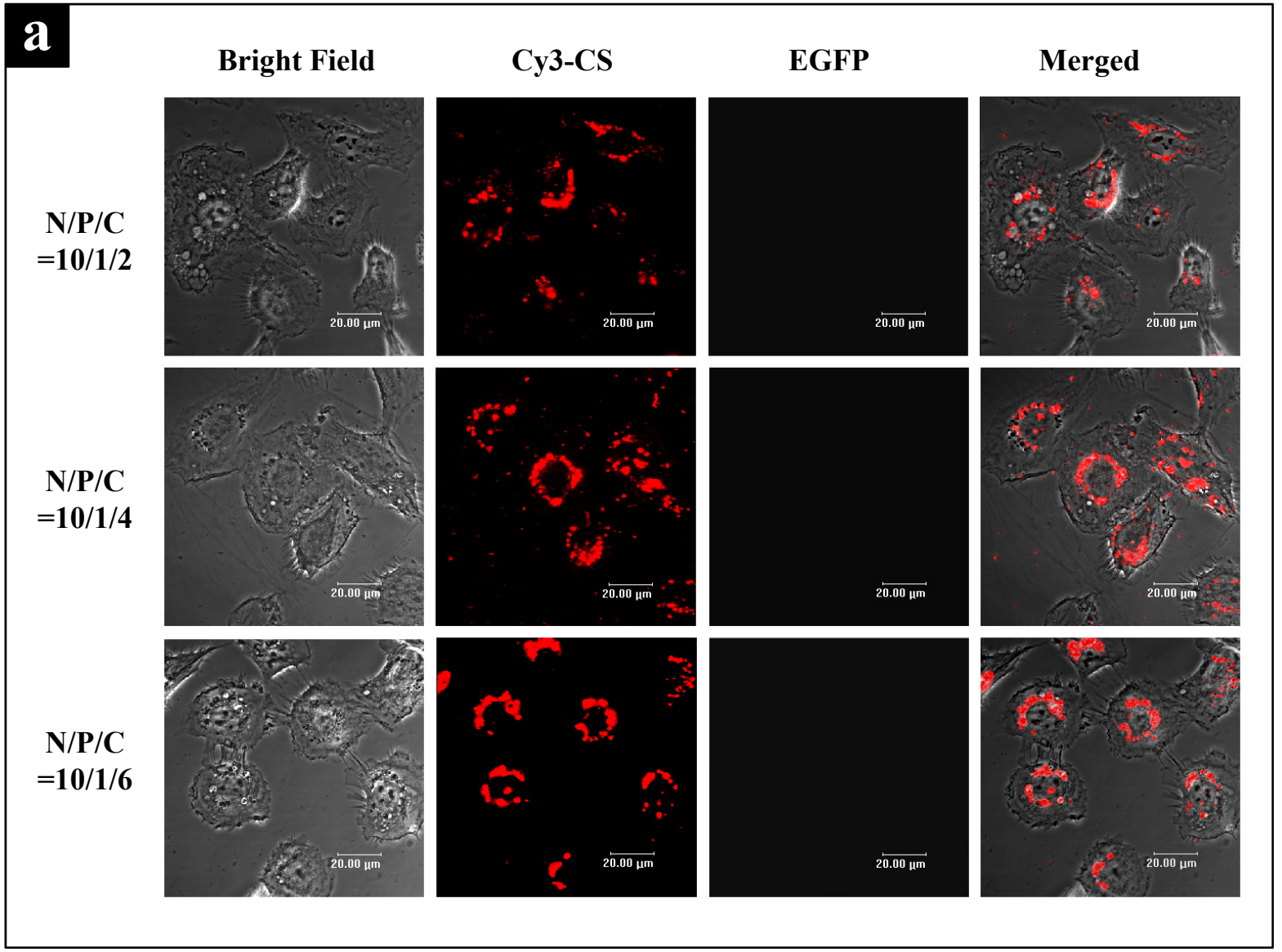

Figure 5b

Figure 5

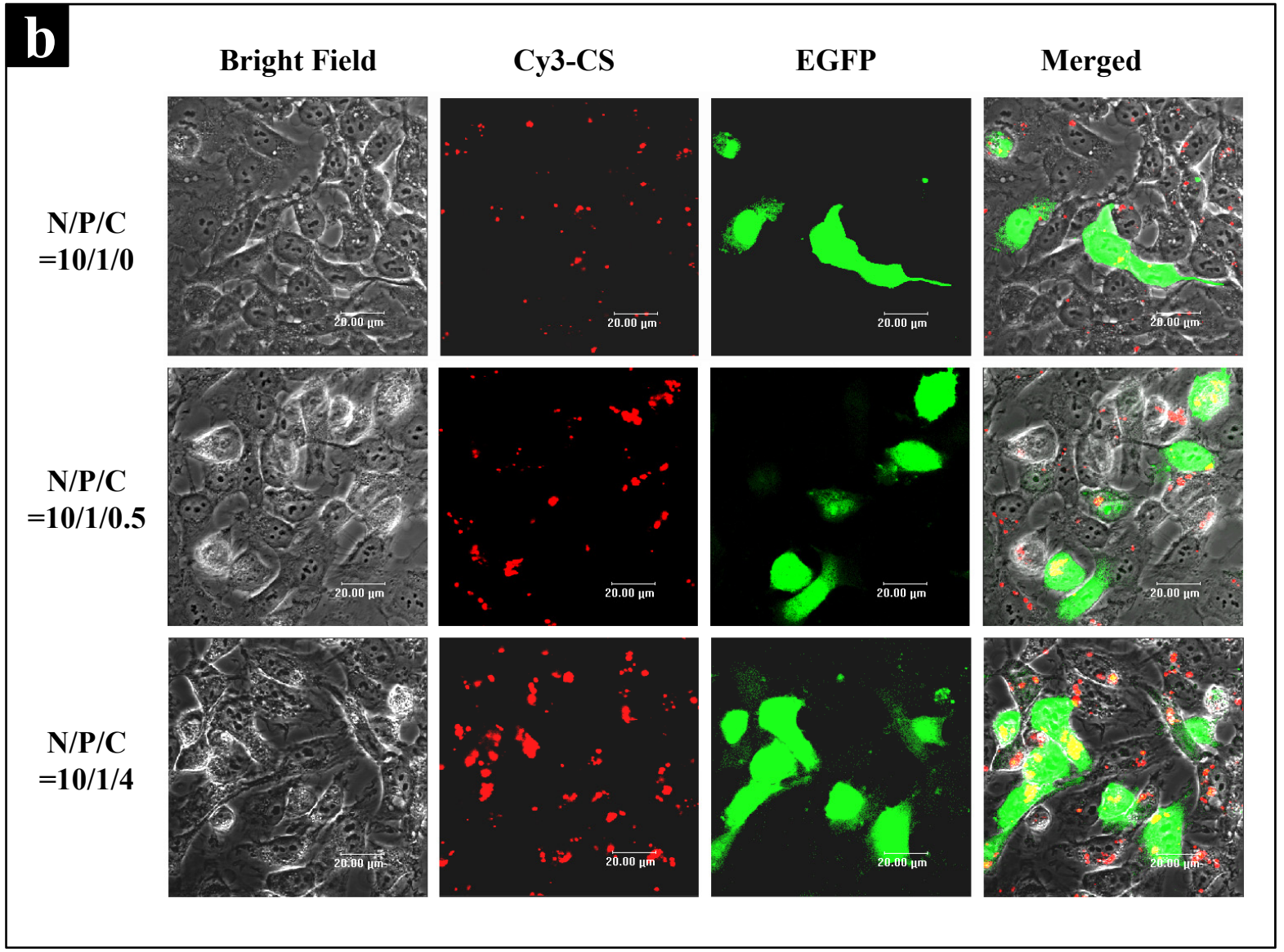

Figure 5c

Figure 5

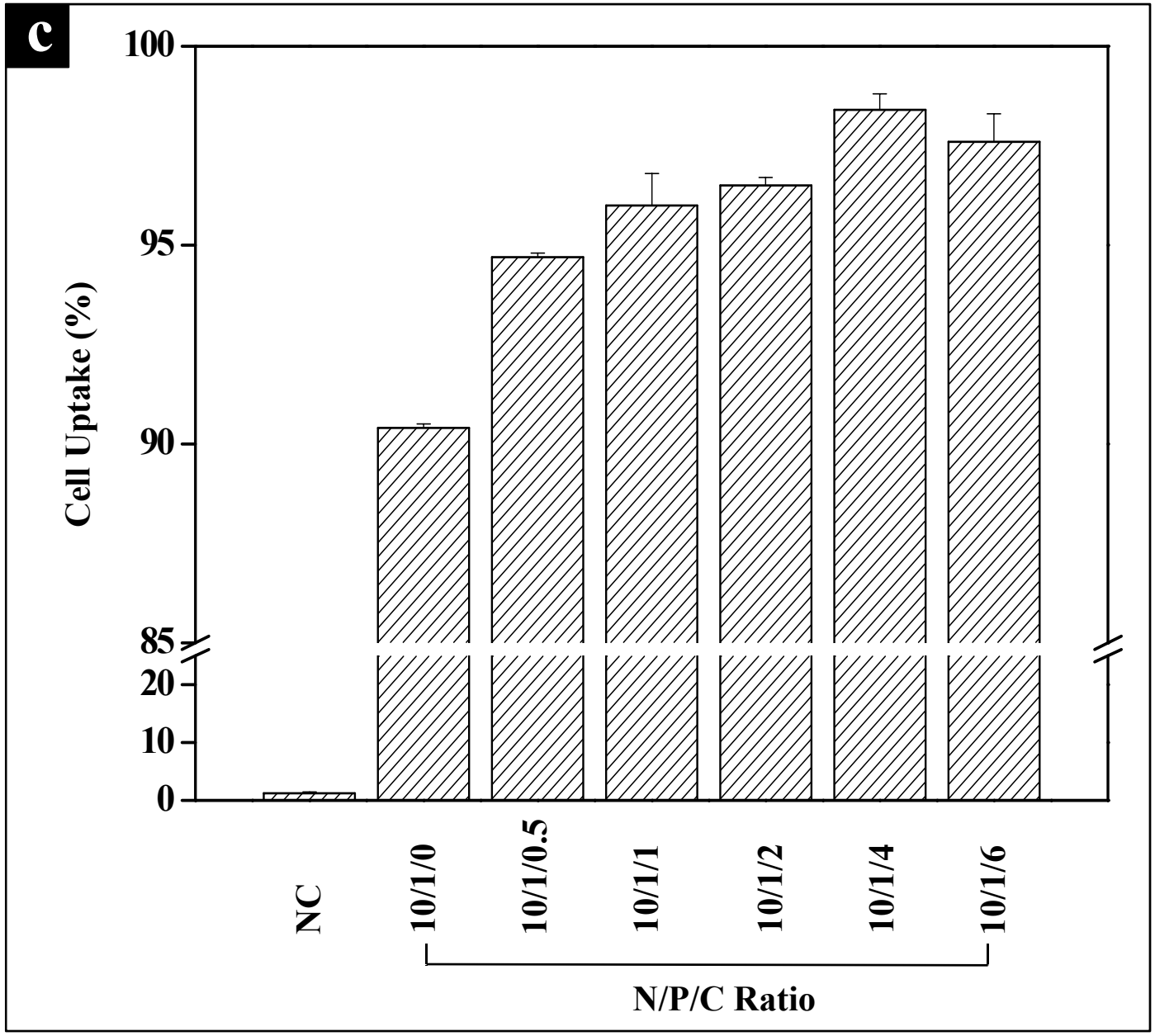

Figure 5d

Figure 5

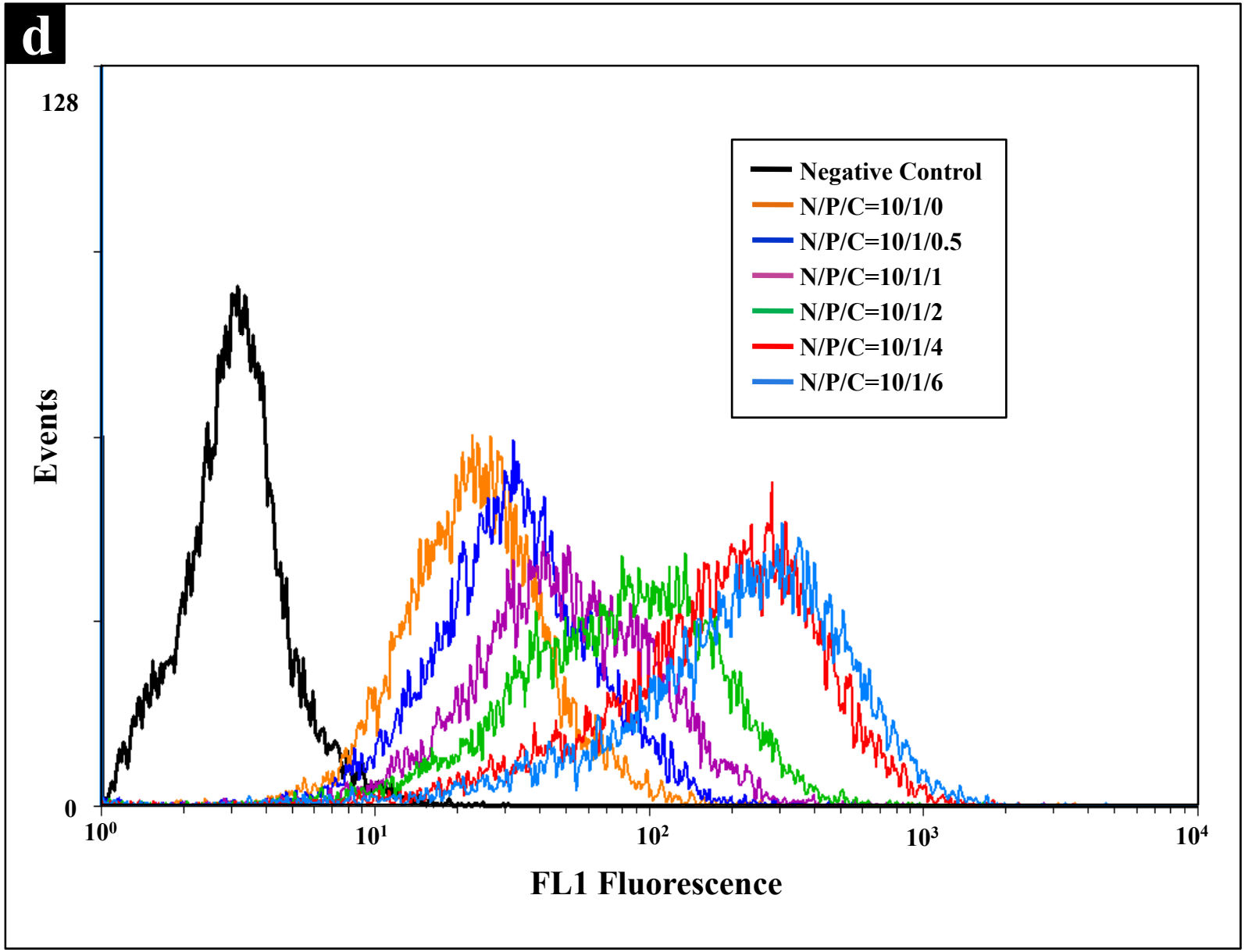

Figure 6

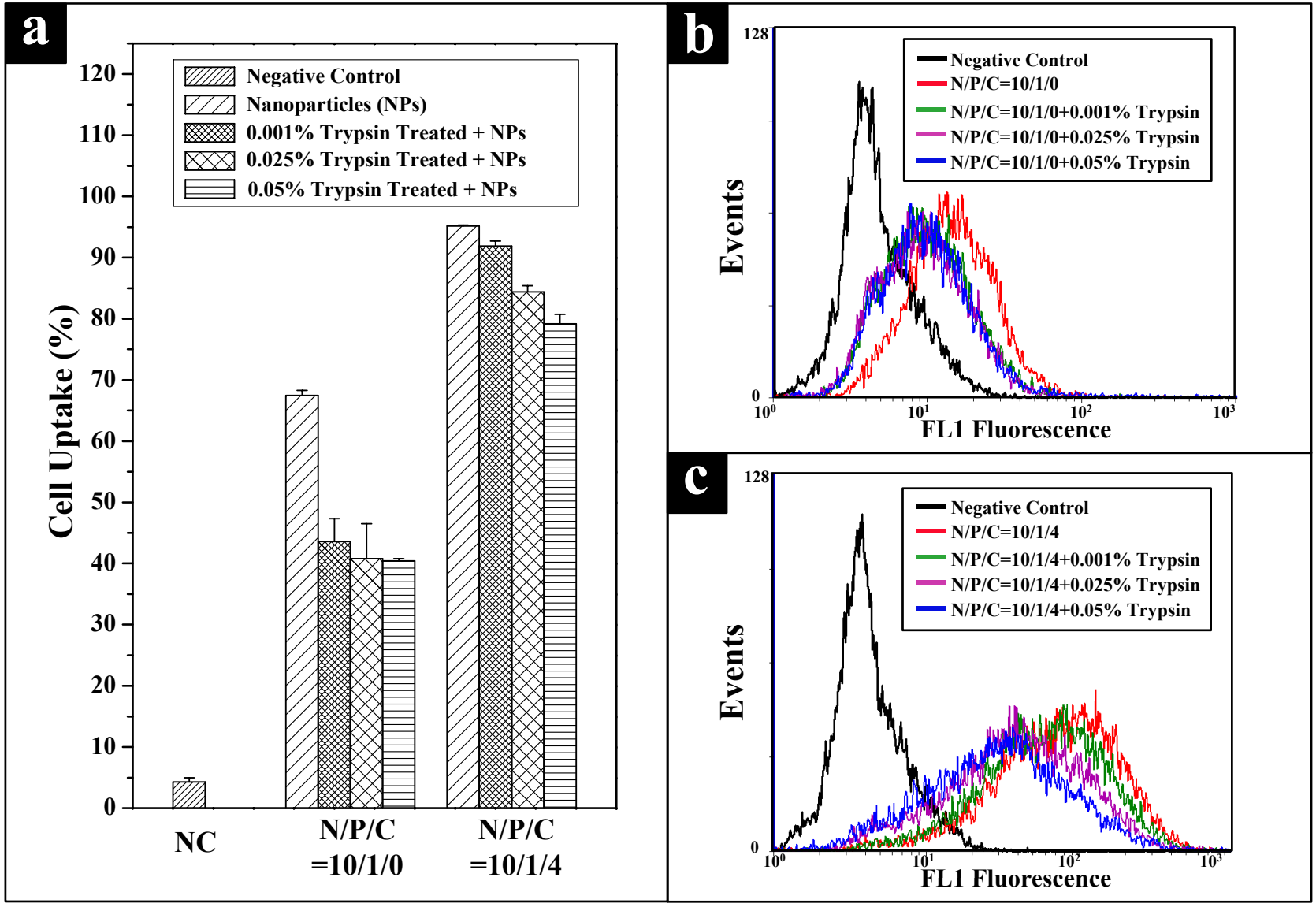
a
Negative Control
Nanoparticles (NPs)
0.001% Trypsin Treated + NPs
0.025% Trypsin Treated + NPs
0.05% Trypsin Treated + NPs
Cell Uptake (%)
0
10
20
30
40
50
60
70
80
90
100
110
120
NC
N/P/C =10/1/0
N/P/C =10/1/4
b
Negative Control
N/P/C=10/1/0
N/P/C=10/1/0+0.001% Trypsin
N/P/C=10/1/0+0.025% Trypsin
N/P/C=10/1/0+0.05% Trypsin
Events
128
0
10^0
10^1
10^2
10^3
FL1 Fluorescence
c
Negative Control
N/P/C=10/1/4
N/P/C=10/1/4+0.001% Trypsin
N/P/C=10/1/4+0.025% Trypsin
N/P/C=10/1/4+0.05% Trypsin
Events
128
0
10^0
10^1
10^2
10^3
FL1 Fluorescence

Figure 7

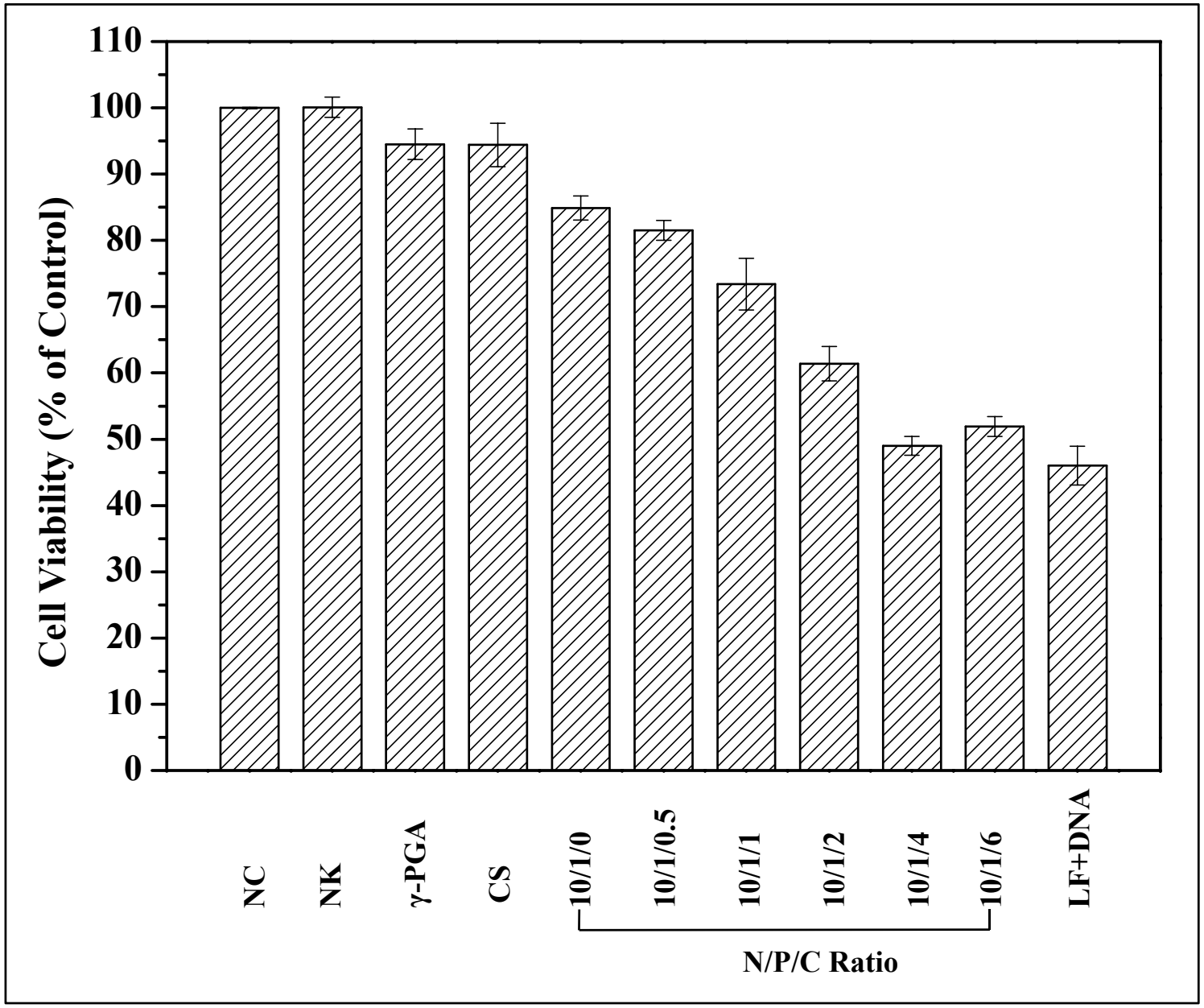
Cell Viability (% of Control)
110
100
90
80
70
60
50
40
30
20
10
0
NC
NK
γ-PGA
CS
10/1/0
10/1/0.5
10/1/1
10/1/2
10/1/4
10/1/6
LF+DNA
N/P/C Ratio

Figure 8a

Figure 8

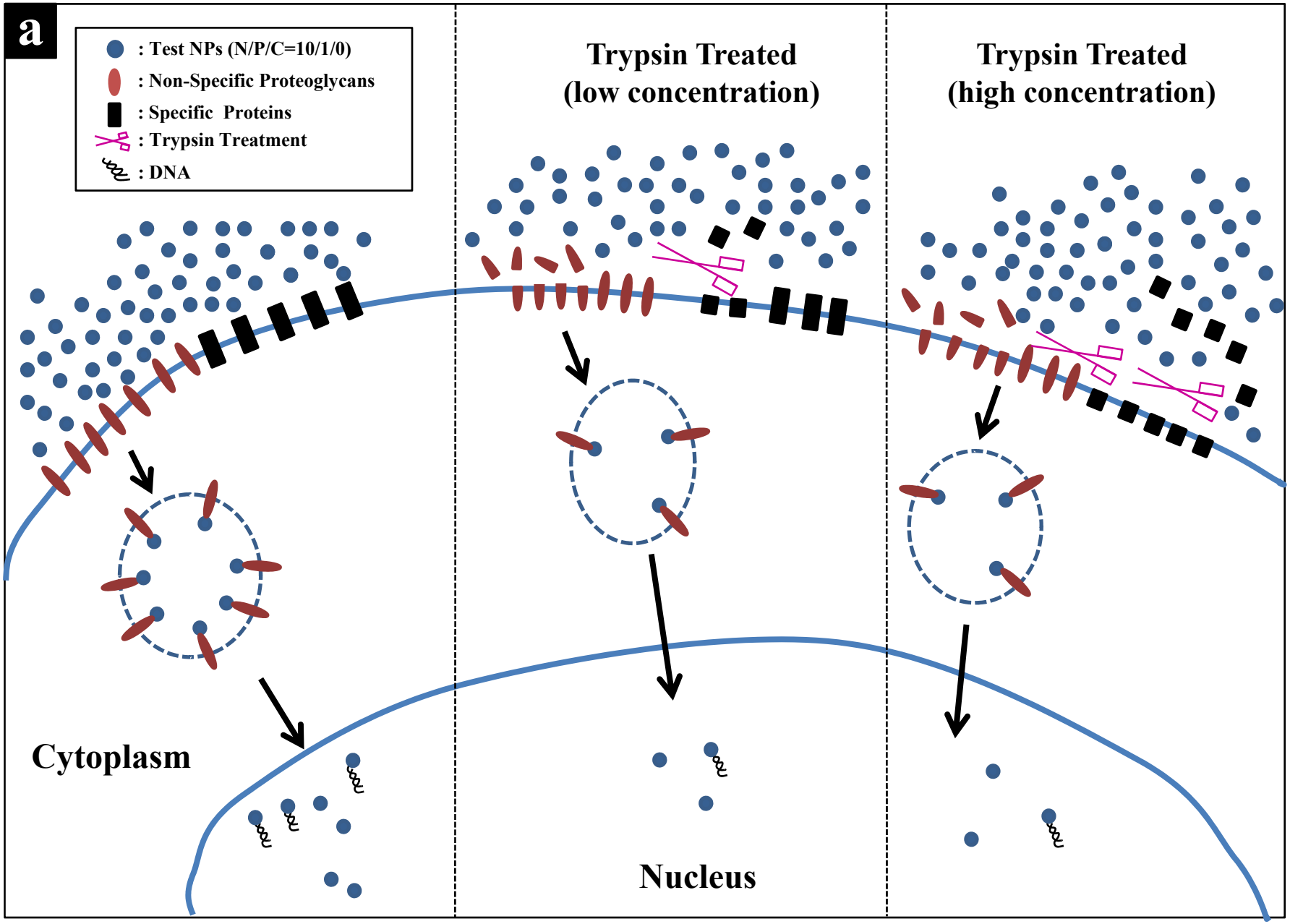

Figure 8b

Figure 8